Study of Water Interaction with UO_2, U_2O_5, and UO_3: Tracking the Unexpected Reduction of Uranium Cations and Characterization of Surface-Bound Hydroxyls

Ghada El Jamal, Thomas Gouder,* Rachel Eloirdi, Hicham Idriss, and Mats Jonsson

ABSTRACT: The interaction of water with the surfaces of metal oxides is important to many fields of research, extending from nuclear science to catalysis to energy and biomedical materials. One intriguing phenomenon is the observation that, for a few oxides, water seems to reduce (not oxidize) the oxide substrate. In this work, ultraviolet photoelectron spectroscopy (UPS) has been used to study the reactions of H_2O with prototype oxide nuclear fuels: UO_2, U_2O_5, and UO_3. On UO_2, water adsorbs largely in a molecular state. On U_2O_5, water partially dissociates at −60 °C, thus forming surface −OH groups, and a fraction of the uranium cations are reduced from U^{5+} to U^{4+}. On UO_3, a similar reduction process is seen (reduction of a fraction of uranium cations from U^{6+} to U^{5+}), albeit less pronounced. The chemisorbed H_2O and −OH states via their molecular orbitals (MOs), $1b_2$, $3a_1$, and $1b_1$ for H_2O and 1σ and 1π for −OH, were further analyzed. The $3a_1-1b_1$ binding energy difference (ΔE) was taken as a measure of the bond strength. It was found to be larger on UO_2 and U_2O_5 (2.9−3.0 eV) than on UO_3 (2.2 eV). The charge state of the surface hydroxyl was found to be related to the $1\pi/1\sigma$ intensity ratio, from which, and in conjunction with the created U 5f states, electron transfer to the conduction band under UPS collection was facilitated by the hole trapping capacity of surface −OH groups, at least in the case of UO_3. An energy band diagram is constructed that may explain the redox process observed on UO_3 under UV photon excitation.

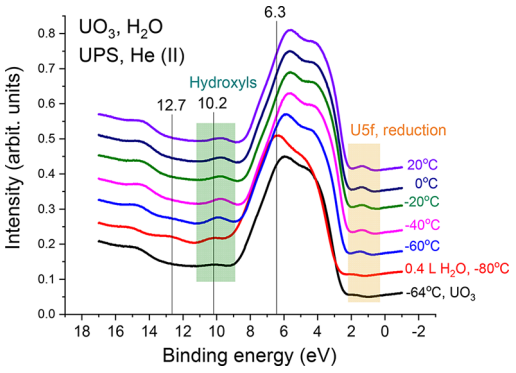

INTRODUCTION

Water interactions with oxides are at the essence of many surface and bulk reactions in natural and applied systems. At the oxide surface, the interaction is governed by two main reactions: acid−base and redox reactions, both of which may occur separately or together. While many studies have addressed water interactions with early transition metal oxides,[1−3] water interactions with actinides have received less attention. Their redox surface character in the presence of water/ice needs particular attention. This would further improve our understanding of electron transfer reactions and is of interest to many applied issues including radiation-induced dissolution of spent nuclear fuel (most spent fuels consist of UO_2, ca. 95%),[4] which contributes to the release and spread of radiotoxic substances. Moreover, little is known about the changes in oxidation states and the associated shift in band energies with respect to adsorbates of the many uranium oxide phases with stoichiometry extending from UO_2 (U^{4+}) to UO_3 (U^{6+}), and virtually none is known for U_2O_5 (U^{5+}). Under reducing conditions that are expected to prevail in groundwaters at repository sites, the UO_2 matrix has very low solubility. The inherent radioactivity of the spent nuclear fuel will induce radiolysis of groundwater and thereby change the redox conditions locally. The oxidizing radiolysis products (primarily $OH^\bullet$ and H_2O_2) will oxidize the surface of UO_2 to, eventually, the considerably more soluble U^{6+}.[5]

Previously, uranium oxide films exposed to H_2O and H_2O/H_2 plasmas under ultrahigh vacuum (UHV) conditions were studied to mimic the effect of water radiolysis in a system where dissolution and precipitation could not occur while the reacted surface was analyzed in situ.[6−8] The uranium oxide films were characterized before and after exposure to the plasmas using X-ray photoelectron spectroscopy (XPS) and ultraviolet photoelectron spectroscopy (UPS). It was found that both the crystal phase and its surface states affected the modes of adsorption. This gives the possibility of studying the nature of surface −OH groups by their valence state. In the past, special attention was given to water interaction with UO_2 single crystals and thin films probed with XPS, in which the

Scheme 1. Preparation Method of the UO_2, U_2O_5, and UO_3 Thin Films

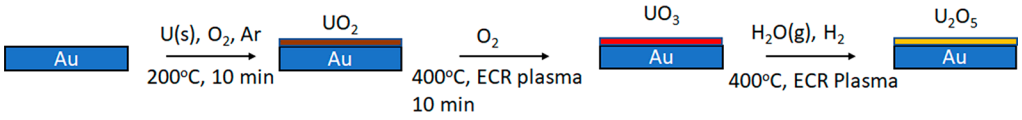

effects of oxygen vacancies were investigated. In these experiments, the oxygen vacancies were created by Ar ion sputtering, and the samples were heated to different temperatures. It was deduced that water dissociated upon adsorption (from XPS O(1s)), H_2 was formed (from temperature-programmed desorption (TPD)), and the surface was subsequently oxidized (from XPS U 4f)[9,10] at temperatures as low as 95 K. In contrast, water was shown to be only weakly adsorbed on stoichiometric UO_2 (111) single crystals (from TPD and low energy electron diffraction (LEED)).[11] The latter experimental results are in broad agreement with density functional theory (DFT) calculations, where the adsorption of water on UO_2 (111) was found to be molecular. Yet, the level of coverage considerably affected the adsorption energy, which ranged from 0.6 eV at 1/4 ML coverage to 2.6 eV at 1 ML coverage (due to hydrogen bonding between molecularly adsorbed water)[12] over the (111) surface. It is not uncommon that partial molecular and dissociative adsorption occurs on oxide surfaces, which gives rise to further adsorbate stabilization.[13−17] Furthermore, XPS and UPS were used to study the interaction of water with PuO_2 films.[18] At low temperatures, water adsorbed mainly dissociatively with small traces in the molecular form. Upon heating the sample under ultraviolet light (with the He II light source during UPS), PuO_2 was found to be reduced into Pu_2O_3. A surface reduction of UO_3 under similar conditions (ice coverage and UV light) was also observed.[19] The possible mechanism was explained as a photocatalytic surface reaction, which takes place when the oxide is excited under UV illumination from the discharge lamp. It is also possible that the ice film (at low temperature) undergoes direct photolysis, and the generated reductants react with the surface.[20−22]

Here, we present a study of the surface reactions of uranium oxide thin films (UO_2, U_2O_5, and UO_3) with H_2O. Information on the adsorbed phase is largely obtained by UPS, as it can probe the molecular orbitals of adsorbates, thus distinguishing among H_2O, −OH, and lattice oxygen (O^{2-}). In addition, it gives direct information about the uranium oxidation state (U^{4+}, U^{5+}, and U^{6+}) from the presence (or absence) of the intensity and width of the U 5f peak. It thus allows for probing into the water adsorption modes together with any possible changes in the uranium cation electronic states.

EXPERIMENTAL SECTION

The starting material, a UO_{2+x} (x < ca. 0.1) thin film, was produced by reactive direct-current sputtering from a uranium target. As a sputter gas, we used a mixture of Ar and O_2. Films were deposited on gold foils (99.99% purity), which were cleaned in situ by Ar ion sputtering and annealed to 200 °C for 10 min before deposition. The plasma in the diode source was maintained by injection of electrons of 25−50 eV energy, which allowed the operation at low sputter gas pressures. To produce stoichiometric $UO_{2.0}$, the initial UO_{2+x} was exposed to atomic hydrogen produced with an electron cyclotron resonance (ECR) plasma source at 400 °C for 10 min, which eliminated potential surplus oxygen, leaving $UO_{2.0}$. UO_3 films were prepared by exposing the UO_2 films to atomic oxygen under the same conditions (i.e., ECR exposure at 400 °C for 10 min). More details on the characterization of the films can be found in ref 23. U_2O_5 films were prepared by reducing the UO_3 films with a mixed plasma of water and hydrogen. The procedure is described in detail in a previous paper (ref 24) and shown in Scheme 1. The content and purity of the films were determined by XPS. The content and purity of the films were determined by XPS. The positions of the U 4f main lines, its full width at half-maximum (fwhm) and the characteristic satellite peaks are a direct probe of the oxidation states of the films.[25]

Thin film deposition, plasma treatment, gas exposure, and data acquisition were carried out in situ. The background pressure was lower than 3×10^{-7} Pa. This ensured the protection of the films from the laboratory atmosphere and any possible external contamination. Low temperatures were reached by cooling the copper sample holder stage using liquid nitrogen. A thermocouple connected to the surface of the films probed the change in temperature throughout the exposure. At the desired temperature, water vapor was introduced via a leak valve, which was connected to a stainless steel pressure container filled with water from a Millipore Milli-Q system for ultrapure water. Water was condensed as a thick ice overlayer on the surface, which later desorbed when the sample was heated.

UPS spectra were taken with He II (40.81 eV) UV light produced by a high intensity windowless discharge lamp. XPS spectra were recorded using monochromatized Al Kα (1486.6 eV) radiation produced by a SPECS μ-focus source. H_2O exposures were done at low temperature (−80 to −150 °C), and the samples were then flashed at increment temperatures, as indicated in the corresponding sections. Ar ion sputtering was conducted using a backfilling method with a pressure of 3×10^{-3} Pa, an Ar beam energy of 1 kV, and an emission current of 10 mA.

RESULTS

UO_2. The UPS spectrum of pristine UO_2 is shown in Figure 1A (black line). It contains the U $5f^2$ emission at 1.8 eV and a broader peak system (4−10 eV) that is attributed to the valence band.[26] The valence band consists of the O 2p and U (5f, 6d, 7s) states. A change in the oxidation state of uranium affects the 5f states, which for U^{4+}, U^{5+}, and U^{6+} contain 2, 1, and 0 electrons, respectively. With U oxidation, the peak centered at ca. 1.8 eV decreases in intensity and finally disappears for UO_3. Its intensity, compared with the valence band, thus gives a good indication of the U oxidation state. It was also found that the 5f shape (fwhm) changes with the oxidation state, as is further discussed below.

After UO_2 is exposed to 0.2 L of water at −115 °C, three peaks appear at the binding energies of 7.2, 9.8, and 13.2 eV relative to the Fermi energy (E_F). These peaks are attributed to the three molecular orbitals of water ($1b_2$, $3a_1$, and $1b_1$).[27] Thus, water adsorbs molecularly on UO_2 at a low dosage.

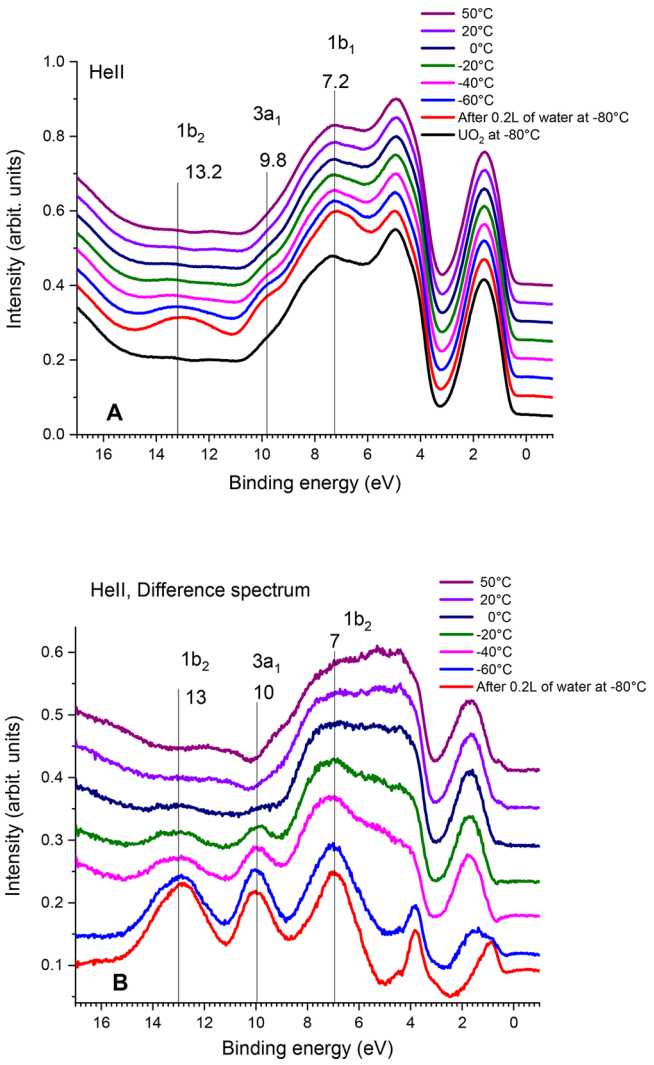

Figure 1. UPS spectra of UO_2 exposed to water. (A) 0.2 langmuir (L) at −80 °C followed by heating (away from the UV light) to the indicated temperatures. (B) Difference spectra of the same series.

When the surface is heated, a gradual decrease of the water signal is observed, as seen in the difference spectra of Figure 1B; by 0 °C, almost all of the water/ice has desorbed. There are only marginal variations in the shape and the intensity of the U 5f peaks. These indicate the low surface coverage (much less than a monolayer) and the fact that water does not oxidize UO_2 (in which case, the 5f emission would have been suppressed and narrowed).

At higher dosages (5 L, Figure 2), water physisorbs at temperatures below ca. −120 °C. The photoemission peaks of the physisorbed water appear at 6.8, 9.9, and ca. 13.0 eV. A thick ice film forms, hiding all oxide lines below (not shown). When the surface is warmed to −60 °C, most physisorbed water desorbs, and only the three small lines of the chemisorbed water ($1b_2$, $3a_1$, and $1b_1$) remain, adding to the O 2p and U 5f oxide lines. At 0 °C, there are some differences between the low (0.2 L) and high (5 L) dosed surfaces. Namely, the presence of the signal attributed to surface hydroxyls at ca. 10 eV is more pronounced at the higher dosage due to a coverage effect. This is either because of dissociative adsorption occurring on inevitable O-defected sites, which must be negligible since no change in the 5f lines is seen, or because of possible non (111)-terminated surfaces that contain alternating rows of O anions and surface cations, such as in a (110) termination (the surface energy of the (110) termination, 1.54 eV, is considerably higher than that of the (111) termination, 0.9 eV).[28]

U_2O_5. Before the results of the water interactions with U_2O_5 are presented, it is worth discussing the core and valence levels of this oxide together with those of UO_2 and UO_3. As mentioned in the Experimental Section, a nearly pure U_2O_5 film composed of only U^{5+} cations has been produced recently.[23] This was made possible by the reduction of UO_3 and not by the oxidation of UO_2. Figure 3 presents XPS U 4f and UPS (He II) of the O 2p−U 5f region, while Tables 1 and 2 show the extracted parameters. The different oxidation states of U cations from +4 to +6 can be distinguished by their satellite structures and, less accurately, by their binding energy positions. U^{6+} has two pairs of satellites at 4.0 and 9.6 eV above their parent U 4f lines. U^{4+} has one pair of satellites at 6.9 eV, and U^{5+} has one pair of satellites at 8.2 eV above their parent U

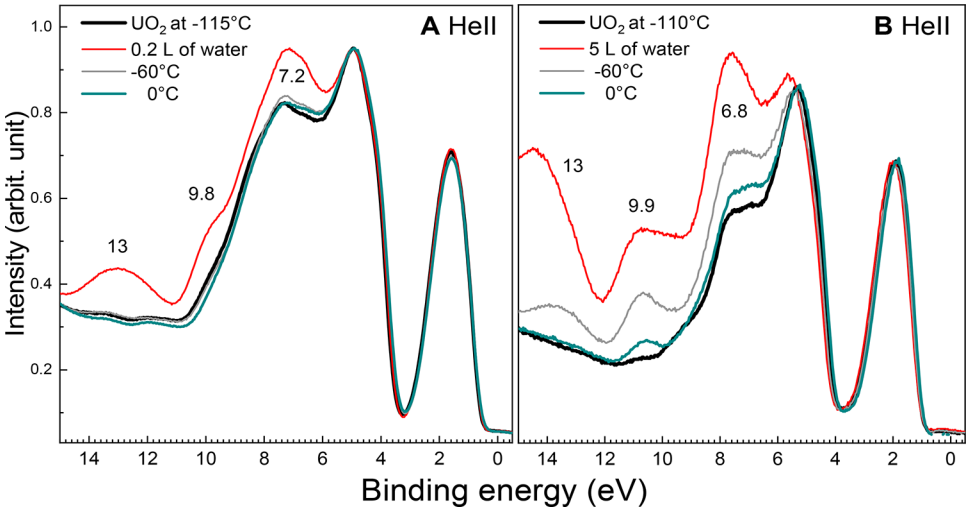

Figure 2. UPS spectra of UO_2 exposed to water. (A) 0.2 langmuir at −115 °C and (B) 5 langmuir at −110 °C. Spectra are taken after exposure and after gradual warming (−60 °C, 0 °C).

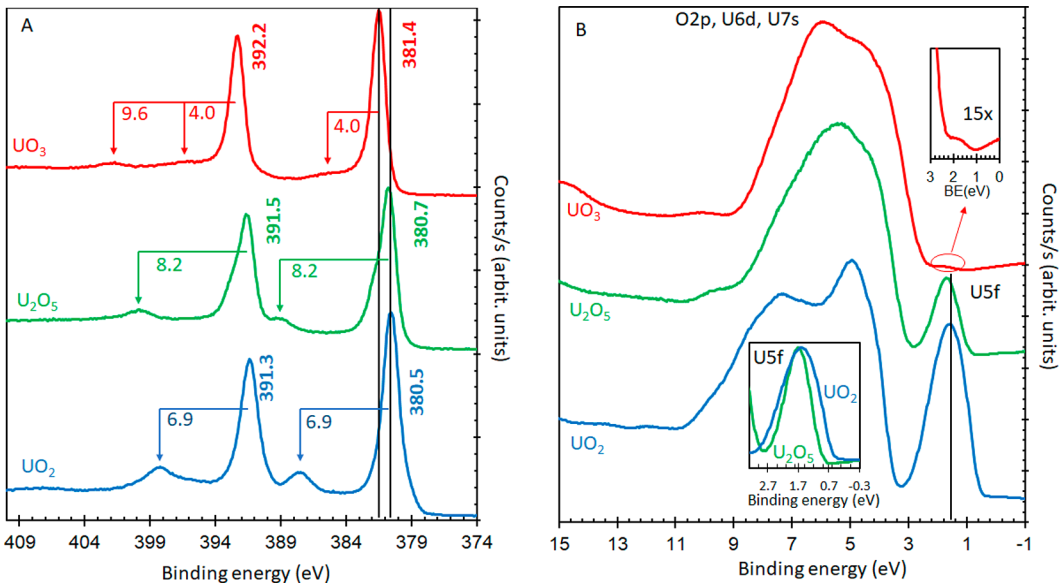

Figure 3. (A) XPS U 4f of the as-prepared UO_2, U_2O_5, and UO_3 thin films. The binding energy positions (in eV) of the $4f_{7/2}$ and $4f_{5/2}$ peaks are indicated, while those of the satellites are pointed at by arrows, with the difference in energy with the parent peaks indicated. (B) UPS (He II) of the as-prepared UO_2, U_2O_5, and UO_3 thin films. The bottom inset is an intensity normalized U 5f to highlight the difference in shape between those of U^{4+} and U^{5+} cations. The top right inset is a 15× magnification of the U 5f region in UO_3, attributed to oxygen defects.

Table 1. XPS U 4f Binding Energy Positions of the As-Prepared UO_2, U_2O_5, and UO_3 Thin Films[a]

XPS lines	UO_2 (eV)	U_2O_5 (eV)	UO_3 (eV)	Δ (S_i − U 4f) (eV)
U $4f_{7/2}$	380.5	380.7	381.4	
U $4f_{5/2}$	391.3	391.5	392.2	
Δ(U $4f_{5/2}$ − U $4f_{7/2}$)	10.8	10.8	10.8	
S_1, S_2	387.4, 398.2			6.9
S_1, S_2		389.0, 399.7		8.2
S_1, S_2, S_3, S_4			385.2, 396.3, -, 401.8	4.0, 9.6

[a]Also shown are the binding energy positions of their satellites, as well as the energy difference between the lines (last column). Note that for the second set of satellites for U^{6+} (S_3 and S_4), the first one (S_3) is not resolved because it is obscured by the U $4f_{5/2}$ peak.

Table 2. UPS (He II) Binding Energy Positions of the As-Prepared UO_2, U_2O_5, and UO_3 Thin Films[a]

	UO_2	U_2O_5	UO_3
U 5f (normalized)	0.236	0.075	-
O 2p (normalized)	1.0	1.0	1.0
fwhm, U 5f (eV)	1.5	1.0	-
fwhm, O 2p (eV)	4.8	4.3	4.3

[a]The normalized peak areas given for U 5f and O 2p are guides to indicate the less pronounced presence of U^{5+} in U_2O_5 when compared to that in UO_2.

4f lines. Close inspection of the U 4f lines of U_2O_5 shows the absence of satellites related to U^{4+} and U^{6+}, yet the peaks have some asymmetry at their high binding energy sides, probably due to the presence of some U^{6+} cations that were not reduced during the preparation. The valence band shows a clear distinction among the three oxides based on the intensity and shape of the U 5f line. In UO_2, a pronounced U 5f signal with a fwhm of 1.5 eV exists at about 1.7−1.8 eV below E_F. Its peak area is about 24% of that of the O 2p band (Table 2). UO_3 shows the near absence of U 5f lines, and traces are still seen, as indicated in the magnified region in Figure 3. These are most likely due to unavoidable oxygen defects. The UPS spectrum of clean U_2O_5 is also composed of the U 5f peak and the O 2p valence band, just as with UO_2. Its U 5f peak is smaller than that of UO_2 when compared to the O 2p band because of the higher oxidation state of U^{5+} with, consequently, a lower 5f count ($5f^1$ for U_2O_5 and $5f^2$ for UO_2); it represents about 8% of the peak area of the O 2p band. Also, the U 5f peak is narrower in U_2O_5 than in UO_2 (see the inset in Figure 3 and Table 2). This is due to the $5f^1$ configuration, which, after photoemission, gives a single final state ($5f^0$) that is narrower than the doublet final state of UO_2 ($5f^1_{5/2}$ and $5f^1_{7/2}$). The shape of the O 2p band is also slightly different than that of UO_2, which is most likely due to the changed band structure in U_2O_5.

When the U_2O_5 film is exposed to 6 L of water at −150 °C, the MO peaks of chemisorbed water appear at 13, 10.1, and 7.4 eV, but the middle peak ($3a_1$) at about 10 eV is larger in this case (see Figures 1 and 2, water on UO_2). This is attributed to the superposition of the $3a_1$ water peak and the 3σ −OH peak. It indicates that part of the adsorbed water on U_2O_5 dissociates. Figure 4A shows the surface that has been exposed to water at −94 °C and then heated at the indicated temperatures, while Figure 4B shows the difference spectra. A gradual decrease of the water signal occurs, and by about 20 °C, the adsorbed water has largely desorbed.

The changes in the intensity of the U 5f peak at the different temperatures up to 200 °C are presented in Figure 4C. Overall,

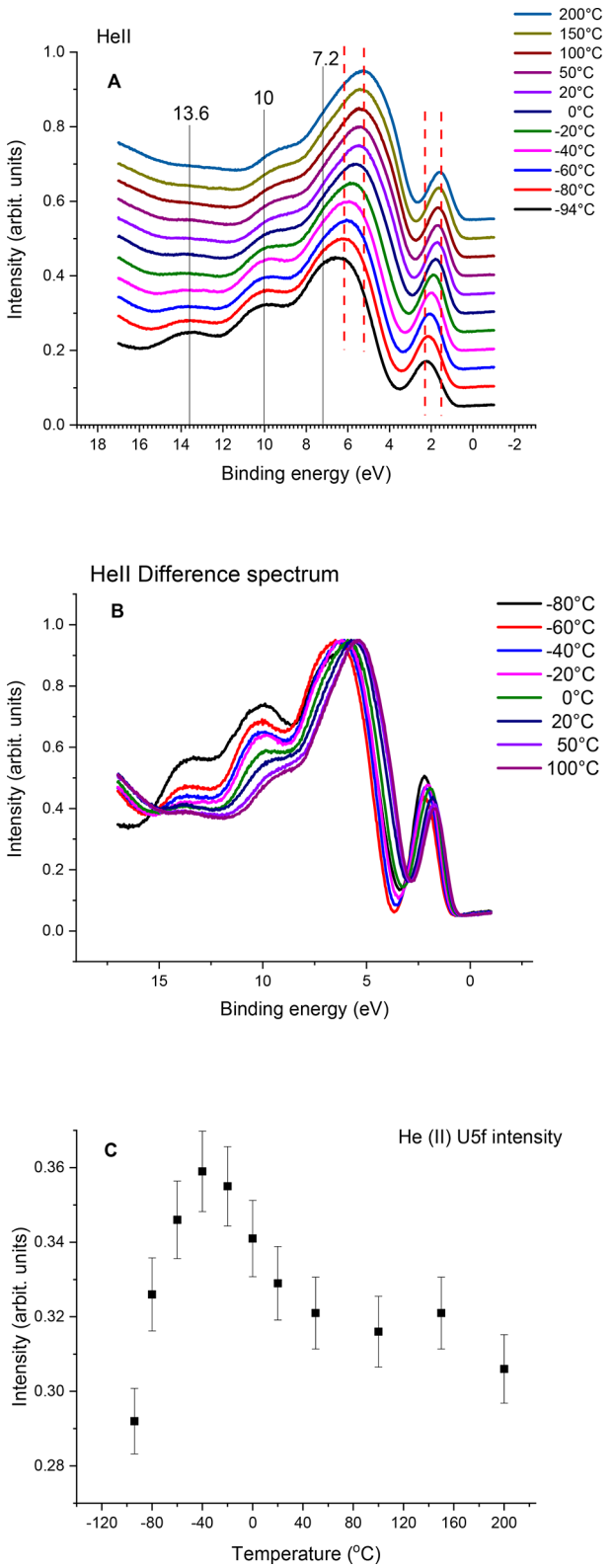

Figure 4. (A) UPS of the valence band of U_2O_5 before and after water adsorption at −80 °C. (B) Difference spectra (unshifted) and (C) the intensity of the U 5f peak at different temperatures.

there is an increase in the signal with an increase in temperature. Yet, the signal goes through a maximum at about −40 °C and then gradually decreases until about room temperature, where it stabilizes thereafter. As mentioned before, evidence of charge transfer in the presence of water has been seen by (and during collection of) UPS of actinide cations.[18,19] To further monitor the observation of Figure 4C, Figure 5 is constructed. There is a difference between the

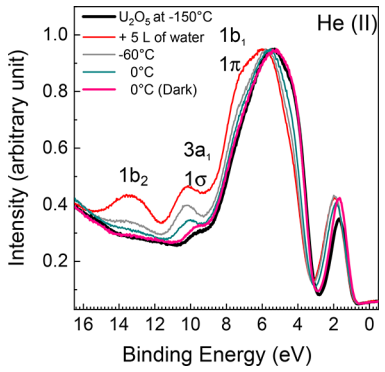

Figure 5. UPS (He II) spectra of U_2O_5 exposed to water at the indicated conditions.

spectra collected from different parts of the sample. When the sample is warmed under UV light, it gives different signals compared to when it is heated in the dark. Under UV light, the U 5f signal is more intense and broad. This indicates a reduction of U_2O_5. Also note that the increase in the 5f signal is concomitant with the appearance of surface hydroxyls. With water exposure, all photoemission lines are shifted to higher binding energies. This collective shift is due to a Fermi-level or work function shift produced by chemisorbed dipoles (OH).

UO_3. In UO_3, uranium has an oxidation state of +6 with all 5f electrons having been transferred to the valence band (O 2p), thereby leaving the U 5f level empty. Therefore, UO_3 has no U 5f signal (Figures 3 and 6) and the shape of the valence band is markedly different than that seen in UO_2.

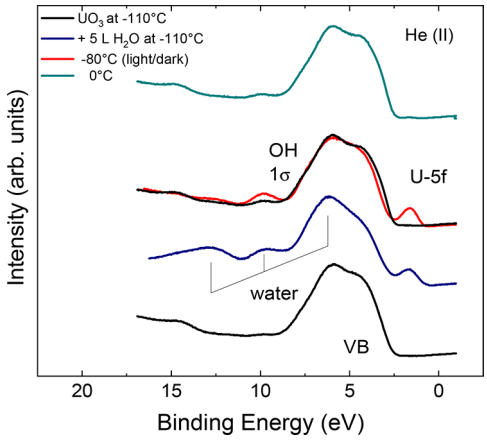

Figure 6. UPS (He II) spectra of UO_3 exposed to 5 L of water at −110 °C.

When the UO_3 film is exposed to 5 L of water at −150 °C, a multilayer film grows (not shown). When the sample is warmed to −110 °C, most of the water disappears and only a small amount stays on the surface, giving weak MO emission lines (Figure 6). Importantly, a weak U 5f line appears at 1.8 eV, indicating that some of the uranium cations are reduced from U^{6+} to lower oxidation states. This spectrum comes from a part of the sample that has been warmed under UV light (in

order to conduct the measurement). When the sample position was changed so that a section of the probed sample was heated in the dark (Figure 6, dark gray spectrum), no reduction was seen. Hence, the reduction that was observed in the first case is a photochemical process (this point will be further considered in the Discussion). Also, as is the case with U_2O_5, the photoreduction goes along with the appearance of a hydroxyl −OH 1σ signal (Figure 7A). It should be noted, however, that even on U^{6+} (dark spot), there is a small −OH 1σ peak.

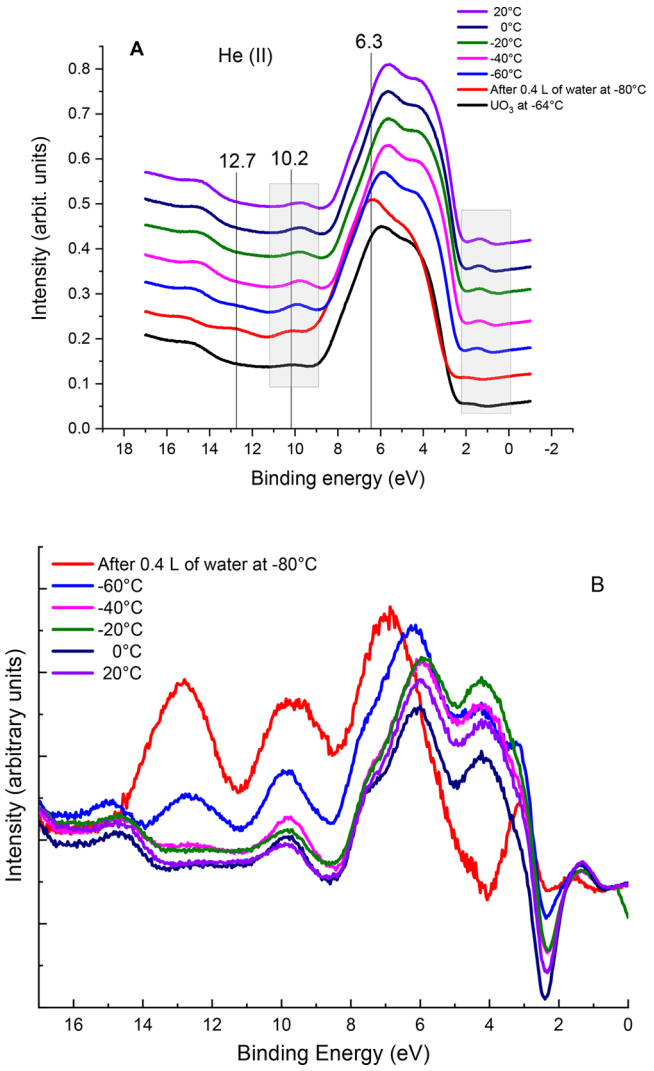

Figure 7. (A) UPS of UO_3 before and after water adsorption at −80 °C, then subsequently heated at the indicated temperatures until 20 °C. (B) Difference spectra of the data presented in (A).

To follow the changes that occur due to the reduction by water under the UV light of He II, a submonolayer exposure to water experiment (0.4 L) was conducted, as seen in Figure 7A,B. The appearance of the U 5f lines together with the persistent signal of the −OH group at 9.9 eV is clear, even upon warming to 20 °C. Figure 7B shows the difference spectra of the same experiment. At −80 °C, the U 5f signal appears and seems to be constant in its intensity and energy position at the investigated temperature (positive signal < 2 eV). Also, the signals at 10 and 12.8 eV remain unshifted. The features of the difference spectra between 7 and 2 eV are complex, as there are contributions from the shift in the work function due to surface coverage and rehybridization between O 2p and U 5f upon reduction.

DISCUSSION

Termination Layer Importance. The nature of the last atomic layer and the crystal structure have an influence on water adsorption, and both depend on the synthesis method. In the present study, polycrystalline films were prepared by sputter deposition at 250 °C and then annealed at 400 °C. The UO_2 films are highly textured, with a preferential orientation of (111).[23] This is in line with fluorite surfaces in general, where (111) is found to be the most stable, followed by (110) and then the reconstructed (100).[29] The termination layer on this face is composed of 3-fold coordinated oxygen atoms.

UO_3 films have been produced by oxidizing the initial UO_2 films in an O plasma. U_2O_5 is produced by the reduction of UO_3 via atomic hydrogen. Water chemisorbs on cations rather than on anions. This is due to an interaction between a Lewis base (lone pair on the oxygen atom of water, O $2p_z$ being part of the $3a_1$ MO of water) and a Lewis acid (the U cation).[30] In general, hydrogen bonding also occurs, particularly when mixed molecular and dissociated modes are involved.[31] Consequently, water chemisorption on oxygen-terminated surfaces is weak. For example, it was observed that water adsorption on a stoichiometric UO_2 (111) single crystal is weak when compared to that on oxygen-deficient UO_2 (111), produced by Ar ion sputtering (preferentially removing the oxygen atoms).[10] This is due to the partial reduction of U^{4+} upon removal of a fraction of the terminal surface oxygen anions. For the three oxides studied here, water is weakly adsorbed (the −OH $1b_2$ signal at 13 eV is weak, indicating a low surface concentration).

To probe this adsorption mode, Figure 8 compares water adsorption on two U oxide surfaces prepared by chemical and physical reduction of UO_3. In the first case, UO_3 has been reduced by being exposed to atomic hydrogen at 400 °C. In this case, reduction proceeds via the reaction of hydrogen atoms with surface oxygen, thereby producing −OH groups. Subsequently, after a second reaction with another hydrogen atom, water is produced, which desorbs due to the high temperature. As such, this reaction is not different from that of reduction using molecular hydrogen, except that the sticking coefficient of the latter is many orders of magnitude smaller than that of a hydrogen atom on metal oxides in general.[32] However, there are subtle differences that are worth mentioning here. Strictly speaking, when bonding with surface oxygen ions, a hydrogen atom is a hydrogen ion and an electron. Because of the ionization potential and electron affinity differences between a hydrogen ion and an oxygen anion, in making an −OH group, the two electrons of the bond originate from the oxygen anion. Therefore, for each −OH group formed, one electron (from each hydrogen atom) goes into the oxide.

$$H^{\bullet} + O_{(surface)}{}^{2-} \rightarrow -OH_{(surface)} + 1e \quad (1)$$

$$2(-OH_{(surface)} + 1e) \rightarrow H_2O \uparrow_{400°C} + V_O + O_{(surface)}{}^{2-} + 2e \quad (2)$$

Here, V_O is an oxygen vacancy, and the H−H bond dissociation energy is 4.44 eV at 298 K.[33]

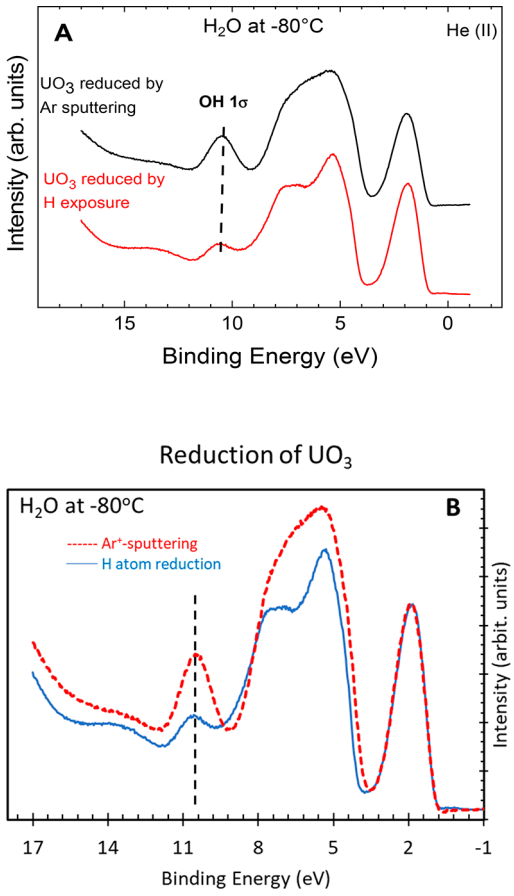

Figure 8. (A) Water adsorption of U oxide surfaces produced by (i) chemical (H exposure) and (ii) physical (Ar ion sputtering/reduction) modification of UO_3. (B) Normalized spectra with respect to the U 5f line intensity.

This is unlike the reaction with molecular hydrogen, where the latter is heterolytically dissociated[34] and, therefore, reduction only occurs when water is removed, leaving behind an oxygen vacancy and two electrons (just as is the case with H atoms). In other words, reduction occurs with H atoms irrespective of water desorption (eq 1), while reduction with molecular hydrogen requires the desorption of water (eq 2 or 3).

$$H_2(g) + O_{(surface)}^{2-} \rightarrow H_2O(g) + V_O + 2e \quad (3)$$

The reduction with H atoms most likely involves hydrogen interatomic diffusion, which results in the reduction of deeper layers. In the absence of a known diffusion coefficient of hydrogen atoms in UO_3, we can make an estimate based on that of UO_2: $D = D_o \exp(-14.3\ \text{kcal}/RT)\ \text{cm}^2/\text{s}$. At 400 °C, D is about $10^{-6}\ \text{cm}^2/\text{s}$ or $10^{10}\ \text{Å}^2/\text{s}$ (with $D_o = 0.037\ \text{cm}^2/\text{s}$).[35] Bulk defects may also act as traps for hydrogen atoms.[36]

In the second case, the surface was bombarded with Ar ions at room temperature. Ar ions preferentially remove oxygen atoms and not uranium atoms due to their mass difference. This is a complex process with a cascade of reactions that are well described by the so-called "Sigmund theory of sputtering".[37] Sputtering efficiency is a function of many parameters, such as the Ar ion flux, the accelerating voltage, and the angle of incidence (all of which affect the extent of ions that penetrate the oxide layers and the associated local heat generated).[38] In this case, the removal of oxygen atoms leaves behind two electrons, as in the case of reduction with two hydrogen atoms. However, hydrogen is not used. As seen in Figure 8, there is a pronounced hydroxyl signal in addition to the appearance of the 5f band and, therefore, all of the signal would originate from water adsorption (neglecting back groundwater contribution).

$$H_2O(g) + V_O + O_{(surface)} \rightarrow 2{-}OH_{(surface)} \quad (4)$$

This reaction (eq 4) is charge-neutral; it does not consume electrons unless molecular hydrogen is formed, and it does not add electrons unless molecular oxygen is formed.

Since water adsorption on fully oxidized surfaces is negligible, then the presence of surface hydroxyls is related to water dissociation on oxygen defects (which may titrate them). In Figure 8, both spectra are normalized to the maximum intensity of the U 5f signal. It is seen that the fwhm of U 5f is the same in both cases. However, water dissociative adsorption is more pronounced on the Ar ion sputtered surface when compared to the surface reduced with H atoms. Because Ar ions (with an energy of 1 kV) are not poised to penetrate deep into the subsurface while H atoms can diffuse into the bulk, the exact difference in the reduction bulk process is not known. It is worth noting the ill-defined nature of the O 2p band of the sputtered surface compared to that of the as-prepared surface. This difference is because Ar ions, in addition to the reduction process, cause surface disorder. This has been observed before on Ar ions sputtered on single crystalline oxide surfaces and noncrystalline powder.[39,40]

Hydroxyl Radicals (−OH•), Hydroxyl Groups (−OH), and a Plausible Band Energy Diagram. Water molecules can have a weak electrostatic interaction (ion−dipole attraction) with the surface in the physisorbed state, or they can exhibit orbital overlap in the chemisorbed state. The ionic nature of metal oxides promotes Lewis acid−base and/or donor−acceptor interactions.[41] Accordingly, the oxygen ions of the surface will act as basic sites and interact with the H^+ of the −OH group of water. The deprotonation of water molecules will produce surface hydroxyl groups on the metal oxide. This is described as a heterolytic dissociative chemisorption according to the reaction below (note that the two −OH groups on the right-hand side of eq 5 are not equivalent):

$$H_2O(g) + \mathbf{O}_{(lattice)}^{2-} \rightarrow -\mathbf{OH}_{(lattice)} + -OH_{(adsorbate)} \quad (5)$$

Figure 9 compares the difference spectra of UO_3 and UO_2 containing surface hydroxyls and adsorbed water molecules. These are produced by exposure to $H^\bullet$ at −80 °C and warming to −60 °C. Both −OH groups and H_2O are present on the surface, and their signals overlap. The spectra were normalized to the $1b_2$ peak intensities of water. It can be seen that the $1b_1/1\pi$ peak is significantly smaller for UO_3. Since the $1b_1$ water contribution can be assumed to be the same in both cases (due to the normalization to the $1b_2$ intensities of water), the difference must be attributed to the 1π being smaller for $-OH/UO_3$ than for $-OH/UO_2$. A possible explanation for this difference would be the charge of the surface on −OH. In −OH, the binding orbital 3σ is constructed by hybridization of the O $2p_z$ and H 1s orbitals, which corresponds to the $3a_1$ of H_2O (Scheme 2). The remaining $2p_x$ and $2p_y$ atomic orbitals are degenerate and essentially nonbonding (even slightly

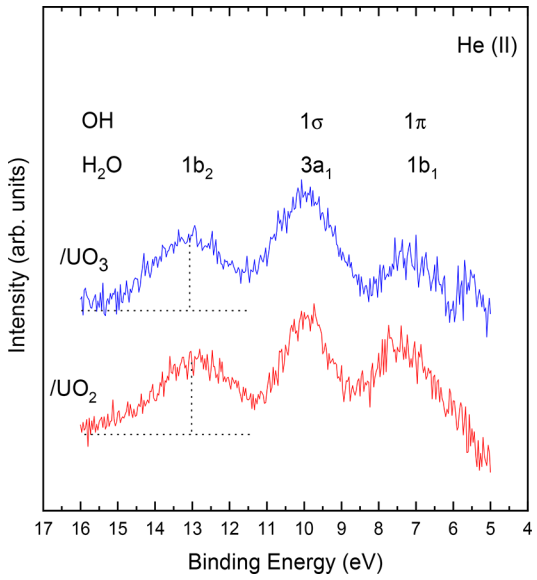

Figure 9. Difference spectra (subtraction of the oxide signal) of UO_2 and UO_3 exposed to atomic hydrogen and warmed to −60 °C.

antibonding). They are at a higher energy (lower binding energy) than the 3σ.

Scheme 2. Molecular Orbitals of a Hydroxyl Group

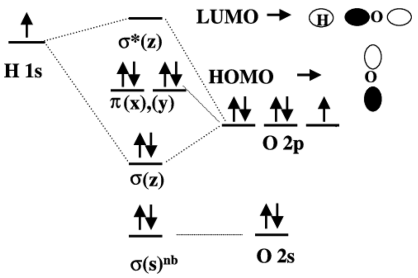

In −OH, the orbitals contain four electrons, while in OH•, they only contain three. These orbitals establish bonding with the surface as π-bonding (between p_x or p_y and the orbitals of the surface atoms).

As seen in Figures 4 and 5 for U_2O_5 and in Figures 6 and 7 for UO_3, under UV light and water, there is a clear presence of U 5f. Scheme 3 presents a possible explanation. To construct this energy diagram, the following points were considered. The valence band (VB) edge energy position of UO_3 is assumed to be marginally different from UO_2 (see ref 42). In the present work, it appears that the VB of UO_3 is slightly lower than that of UO_2; this has been neglected. From the work function of UO_2 (ca. 6 eV) and the standard hydrogen electrode energy position with respect to the vacuum level (−4.44 eV), it is possible to position the conduction band and redox potentials of water to hydrogen.[43] Although we do see shifts in the UPS spectra in the presence of water, band bending was also omitted for simplicity. The stability of the created reduced state (5f) in the case of UO_3 (and U_2O_5) indicates that the system has reached a steady-state condition in the presence of water at −60 °C. In line with the difference observed of the 1π of the −OH groups between UO_3 and UO_2, as indicated above, and the creation of 5f electrons upon UV excitation, it is postulated that surface −OH groups inject electrons into the VB (to trap the holes) and, thus, further stabilize the

Scheme 3. Diagram of Electron Transfer under UV Light Excitation of UO_3, on Which a Layer of Water Is Present at −60 °C[a]

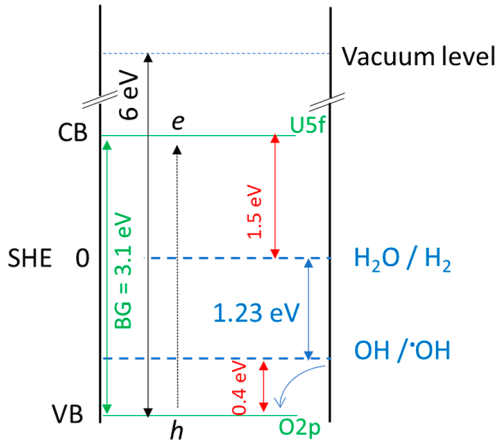

[a]The computed, at the DFT/HF hybrid method (HSE06, that is known to give accurate band gap for early transition metal based oxide semiconductors), band gap and edges of UO_3 changes with its crystallographic structure, and it is between 3 and 3.2 for α and γ UO_3. The measured optical band gap of UO_3 is 2.6 eV (from refs 21 and 42).

conduction band electrons. The −OH groups would then have the character of a more neutral (i.e., less anionic) species and would, therefore, correspond more closely to an adsorbed −OH• (−OH• radicals are usually analyzed after trapping them[44,45] or upon desorption[46]). As a consequence of this hole trapping, electrons under light excitation that have been transferred from the valence band (largely O 2p) to the conduction band (U 5f) are more stable, and the reduction of U^{6+} to U^{5+} in UO_3 or U^{5+} to U^{4+} in U_2O_5 occurs, as seen experimentally in Figures 4−7.

Molecular Orbitals (MOs) of Chemisorbed Water. The MO emission lines of water give information on the change of intramolecular and intermolecular (here, with the surface) bond strengths upon adsorption by the energy difference of the involved molecular orbitals.

(i) The $1b_1$ MO (lone pair on O) does not participate in bonding, neither in intramolecular bonding nor between the molecule and the surface. This is the O $2p_x$ orbital, perpendicular to the HOH plane and parallel to the surface. It is taken as the reference level.

(ii) The $3a_1$ participates most strongly in bonding to the surface. It contains the O $2p_z$ orbital, oriented along the molecular axis and perpendicular to the surface. It gives water its Lewis base character.

(iii) The $1b_2$ is formed with the $2p_y$ orbital (in the molecular plane), overlapping with the H 1s orbitals. It is the main intramolecular bonding orbital and participates little in bonding to the surface.

Upon strong bonding to the surface, the $3a_1$ orbital should be stabilized, and its binding energy and, consequently, its $\Delta E_{3a1-1b1}$ increase. Upon the increase of the intramolecular bond strength, the $1b_2$ binding energy and, consequently, $\Delta E_{1b2-1b1}$ increase. Figure 10 compares the MO spectra of water chemisorbed on UO_2 to that of water/ice on UO_2. For the chemisorbed water, the UO_2 substrate background (its VB) was subtracted. The ice spectrum was shifted to have the $1b_1$ reference line overlap with that of the chemisorbed water. The

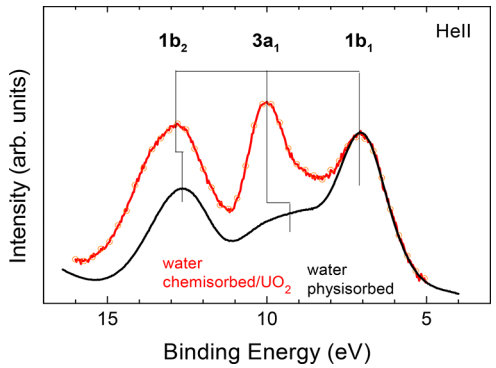

Figure 10. MO lines for water chemisorbed on UO_2 and for multilayer (ice) water on UO_2.

two $1b_1$ lines superimpose remarkably well. The strong intensity increase of $3a_1$ is surprising; this is not due to 1σ of the −OH superimposing onto the water signal, as the corresponding 1π is missing. However, it may instead be due to the increase of the cross section upon mixing with the U f/d states (covalent mixing), or an increased lifetime of the photohole because of solid-state screening. A similar intensity increase was also observed for water adsorbed on $SrTiO_3$.[47]

Upon bonding to the surface, $\Delta E_{3a1-1b1}$ increases considerably to 2.9 eV. This value is lower than that of rutile TiO_2 (110) and perovskite $SrTiO_3$ (100), whose $\Delta E_{3a1-1b1}$ values are 3.5 and 3.2 eV, respectively, and higher than that of rutile SnO_2 (110), whose $\Delta E_{3a1-1b1}$ is 2.6 eV. The intramolecular bond strength also increases upon adsorption, as reflected by an increase of $\Delta E_{1b2-1b1}$ to 5.9 eV. However, this increase is weaker in comparison to that of rutile TiO_2 (110), perovskite $SrTiO_3$ (100), and rutile SnO_2 (110), whose $\Delta E_{1b2-1b1}$ values are 6.2, 6.2, and 6.1 eV, respectively.

Table 3 compares the MOs for water adsorbed on the three oxides. Based on $\Delta E_{3a1-1b1}$, one expects the adsorption energy

Table 3. Molecular Orbital Emissions for Water Adsorbed on UO_2, U_2O_5, and UO_3

	$1b_{1f}$	$3a_1$	$1b_2$	$3a_1-b_1$	$1b_2-b_1$
UO_2	7.1	10.0	12.0	2.9	5.9
U_2O_5	7.4	10.4	13.3	3.0	5.9
UO_3	6.6	8.8	12.6	2.2	6.0

of water to be lowest on UO_3. The intramolecular bond strength does not seem to vary among the three oxides.

CONCLUSIONS

The adsorption modes of H_2O on UO_2, U_2O_5, and UO_3 have been studied by UPS (He II). These three oxides present uranium in different oxidation states (+4, +5, and +6, respectively).

On UO_2, water adsorbs molecularly, as seen by the three emission lines $1b_2$, $3a_1$, and $1b_1$. Surface hydroxyl formation shown by the 1π (superimposing to the $3a_1$) does not take place. On U_2O_5, water partially dissociates, forming surface −OH. Uranium is reduced from U^{5+} to U^{4+} only under UV excitation and the presence of adsorbed water. Reduction is, therefore, a photoinitiated process that involves hole trapping by surface hydroxyls and electron transfer to the metal cations. Atomic hydrogen reduces UO_3 by forming −OH species, while Ar ion sputtering reduces UO_3 directly and, thus, the formation of −OH groups is a consequence (not a signature) of the reduction.

UPS (He II) has been used to characterize chemisorbed H_2O and −OH via their molecular orbitals (MOs). The weak intensity of the −OH group 1π may be an indication of some hydroxyl radical properties when binding to U^{5+} of U_2O_5 when compared to UO_2. Lastly, the chemisorption strength obtained from $\Delta E_{3a1-1b1}$ of the three oxides was extracted and compared to one another. It was found that UO_3 has the weakest adsorption strength (2.2 eV) when compared to UO_2 and U_2O_5.

AUTHOR INFORMATION

Corresponding Author

Thomas Gouder − *European Commission, Joint Research Centre, DE-76215 Karlsruhe, Germany*;
Email: Thomas.GOUDER@ec.europa.eu

Authors

Ghada El Jamal − *School of Engineering Sciences in Chemistry, Biotechnology and Health (CBH), Department of Chemistry, Applied Physical Chemistry, KTH Royal Institute of Technology, SE-100 44 Stockholm, Sweden*

Rachel Eloirdi − *European Commission, Joint Research Centre, DE-76215 Karlsruhe, Germany*

Hicham Idriss − *European Commission, Joint Research Centre, DE-76215 Karlsruhe, Germany; Institute of Functional Interfaces (IFG), Karlsruhe Institute of Technology (KIT), DE-76215 Karlsruhe, Germany*; orcid.org/0000-0001-8614-7019

Mats Jonsson − *School of Engineering Sciences in Chemistry, Biotechnology and Health (CBH), Department of Chemistry, Applied Physical Chemistry, KTH Royal Institute of Technology, SE-100 44 Stockholm, Sweden*; orcid.org/0000-0003-0663-0751

Notes

The authors declare no competing financial interest.

ACKNOWLEDGMENTS

The authors thank Mr. Frank Huber for his technical assistance. H.I. thanks the German Research Foundation (DFG), Project 426888090 - SFB 1441.

REFERENCES

(1) Mu, R.; Zhao, Z.-J.; Dohnálek, Z.; Gong, J. Structural motifs of water on metal oxide surfaces. *Chem. Soc. Rev.* **2017**, *46*, 1785−1806.

(2) Sterrer, M.; Nilius, N.; Shaikhutdinov, S.; Heyde, M.; Schmidt, T.; Freund, H.-J. Interaction of water with oxide thin film model systems. *J. Mater. Res.* **2019**, *34*, 360−378.

(3) Chen, J.; Hope, M. A.; Lin, Z.; Wang, M.; Liu, T.; Halat, D. M.; Wen, Y.; Chen, T.; Ke, X.; Magusin, P. C. M. M.; et al. Interactions of Oxide Surfaces with Water Revealed with Solid-State NMR Spectroscopy. *J. Am. Chem. Soc.* **2020**, *142*, 11173−11182.

(4) Processing of Used Nuclear Fuel, World Nuclear Association. Accessed March 17, 2023. https://world-nuclear.org/information-library/nuclear-fuel-cycle/fuel-recycling/processing-of-used-nuclear-fuel.aspx.

(5) Valsami-Jones, E.; Ragnarsdóttir, K. Y. Solubility of Uranium Oxide and Calcium Uranate in Water, and $Ca(OH)_2$-bearing Solutions. *Radiochim. Acta* **1997**, *79*, 249−257.

(6) Jamal, G. E.; Gouder, T.; Eloirdi, R.; Jonsson, M. Monitoring the gradual change in oxidation state during surface oxidation or reduction of uranium oxides by photoemission spectroscopy of the 5f states. *J. Nucl. Mater.* **2022**, *560*, 153504.
(7) El Jamal, G.; Gouder, T.; Eloirdi, R.; Jonsson, M. Time-dependent surface modification of uranium oxides exposed to water plasma. *Dalton Trans.* **2021**, *50*, 4796−4804.
(8) El Jamal, G.; Gouder, T.; Eloirdi, R.; Jonsson, M. X-Ray and ultraviolet photoelectron spectroscopy studies of Uranium(IV),(V) and(VI) exposed to H_2O plasma under UHV conditions. *Dalton Trans.* **2021**, *50*, 729−738.
(9) Senanayake, S. D.; Waterhouse, G. I. N.; Chan, A. S. Y.; Madey, T. E.; Mullins, D. R.; Idriss, H. The reactions of water vapour on the surfaces of stoichiometric and reduced uranium dioxide: A high resolution XPS study. *Catal. Today* **2007**, *120* (2), 151−7.
(10) Senanayake, S. D.; Waterhouse, G. I. N.; Chan, A. S. Y.; Madey, T. E.; Mullins, D. R.; Idriss, H. Probing Surface Oxidation of Reduced Uranium Dioxide Thin Film Using Synchrotron Radiation. *J. Phys. Chem. C* **2007**, *111* (22), 7963−70.
(11) Senanayake, S. D.; Idriss, H. Water reactions over stoichiometric and reduced UO_2(111) single crystal surfaces. *Surf. Sci.* **2004**, *563* (1), 135−44.
(12) Bo, T.; Lan, J.-H.; Zhao, Y.-L.; Zhang, Y.-J.; He, C.-H.; Chai, Z.-F.; Shi, W.-Q. First-principles study of water adsorption and dissociation on the UO_2 (111), (110) and (100) surfaces. *J. Nucl. Mater.* **2014**, *454*, 446−454.
(13) Hejduk, P.; Szaleniec, M.; Witko, M. Molecular and dissociative adsorption of water at low-index V_2O_5 surfaces: DFT studies using cluster surface models. *J. Mol. Catal. A: Chemical* **2010**, *325*, 98−104.
(14) Bredow, T.; Jug, K. Theoretical investigation of water adsorption at rutile and anatase surfaces. *Surf. Sci.* **1995**, *327*, 398−408.
(15) Lindan, P. J. D.; Harrison, N. M.; Gillan, M. Mixed Dissociative and Molecular Adsorption of Water on the Rutile (110) Surface. *J. Phys. Rev. Lett.* **1998**, *80*, 762−765.
(16) Tian, X.-F.; Wang, H.; Xiao, h.-X.; Gao, T. Adsorption of water on UO_2 (111) surface: Density functional theory calculations. *Comput. Mater. Sci.* **2014**, *91*, 364−371.
(17) Rao, R. R.; Kolb, M. J.; Hwang, J.; Pedersen, A. F.; Mehta, A.; You, H.; Stoerzinger, K. A.; Feng, Z.; Zhou, H.; Bluhm, H.; Giordano, L.; et al. Surface Orientation Dependent Water Dissociation on Rutile Ruthenium Dioxide. *J. Phys. Chem. C* **2018**, *122*, 17802−17811.
(18) Seibert, A.; Gouder, T.; Huber, F. Interaction of PuO_2 thin films with water. *Radiochim. Acta* **2010**, *98*, 647−654.
(19) Gouder, T.; Shick, A. B.; Huber, F. Surface Interaction of PuO_2, UO_2 and UO_3 with Water Ice. *Top. Catal.* **2013**, *56* (12), 1112−20.
(20) Bo, T.; Lan, J.-H.; Zhao, Y.-L.; Zhang, Y.-J.; He, C.-H.; Chai, Z.-F.; Shi, W.-Q. First-principles study of water adsorption and dissociation on the UO_2 (111), (110) and (100) surfaces. *J. Nucl. Mater.* **2014**, *454* (1), 446−54.
(21) Tegner, B. E.; Molinari, M.; Kerridge, A.; Parker, S. C.; Kaltsoyannis, N. Water Adsorption on AnO_2 {111}, {110}, and {100} Surfaces (An = U and Pu): A Density Functional Theory + U Study. *J. Phys. Chem. C* **2017**, *121* (3), 1675−82.
(22) Wellington, J. P. W.; Kerridge, A.; Austin, J.; Kaltsoyannis, N. Electronic structure of bulk AnO_2 (An = U, Np, Pu) and water adsorption on the (111) and (110) surfaces of UO_2 and PuO_2 from hybrid density functional theory within the periodic electrostatic embedded cluster method. *J. Nucl. Mater.* **2016**, *482*, 124−34.
(23) El Jamal, G.; Gouder, T.; Eloirdi, R.; Tereshina-Chitrova, E.; Horákd, L.; Jonsson, M. Mixed H_2O/H_2 plasma-induced redox reactions of thin uranium oxide films under UHV conditions. *Dalton Trans.* **2021**, *50*, 12583−12591.
(24) Gouder, T.; Eloirdi, R.; Caciufo, R. Direct observation of pure pentavalent uranium in U_2O_5 thin films by high resolution photoemission spectroscopy. *Sci. Reports* **2018**, *8* (8306), 1−7.
(25) Al-Salik, Y.; Al-Shankiti, I.; Idriss, H. Core level spectroscopy of oxidized and reduced $Ce_xU_{1-x}O_2$ materials. *J. Electron Spectros. & Relat Phenomena* **2014**, *194*, 66−73.
(26) Nagele, J. R.; J. Ghijsen, J. In *Actinides − Chemistry and Physical Properties, Structure and Bonding*; Manes, L., Ed.; Springer-Verlag, Berlin, 1985, p 197.
(27) Henderson, M. A. The interaction of water with solid surfaces: fundamental aspects revisted. *Surf. Sci. Rep.* **2002**, *46*, 1−308.
(28) Idriss, H. The Surface Reactions of Uranium Oxides. *Surf. Sci. Reports* **2010**, *65*, 67−109.
(29) Tasker, W. The surface properties of uranium dioxide. *Surf. Sci.* **1979**, *87*, 315−325.
(30) Calatayud, M.; Markovits, A.; Menetrey, M.; Mguig, B.; Minot, C. Adsorption on perfect and reduced surfaces of metal oxides. *Catal. Today* **2003**, *85*, 125−143.
(31) Thiel, P. A.; Madey, T. The interaction of water with solid surfaces: fundamental aspects. *Surf. Sci. Rep.* **1987**, *7*, 211−385.
(32) Kunat, M.; Burghaus, U.; Wöll, Ch Adsorption of hydrogen on the polar O−ZnO surface: a molecular beam study. *Phys. Chem. Chem. Phys.* **2003**, *5*, 4962−4967.
(33) Herzberg, G. The dissociation energy of the hydrogen molecule. *J. Mol. Spectrosc.* **1970**, *33*, 147−168.
(34) Griffin, G. L.; Yates, J. T. Adsorption studies of H_2 isotopes on ZnO:Coverage-induced IR frequency shifts and adsorbate geometry. *J. Chem. Phys.* **1982**, *77*, 3744−3750.
(35) Wheeler, V. J. The diffusion and solubility of hydrogen in uranium dioxide single crystal. *J. Nucl. Mater.* **1971**, *40*, 189−194.
(36) Flitcroft, J. M.; Molinari, M.; Brincat, N. A.; Williams, N. R.; Storr, M.; Allen, G. C.; Parker, S. C. The critical role of hydrogen on the stability of oxyhydroxyl defect clusters in uranium oxide. *J. Mater. Chem. A* **2018**, *6*, 11362−11369.
(37) Sigmund, P. Theory of Sputtering. I. Sputtering Yield of Amorphous and Polycrystalline Targets. *Phys, Rev.* **1969**, *184*, 383−416.
(38) Idriss, H.; Barteau, M. A. Characterization of TiO_2 surfaces active for novel organic syntheses. *Catal. Lett.* **1994**, *26*, 123−139.
(39) Kräuter, J.; Mohrhusen, L.; Thiedemann, T.; Willms, M.; Al-Shamery, K. Activation of Small Organic Molecules on Ti^{2+}- Rich TiO_2 Surfaces: Deoxygenation vs. C−C Coupling. *Z. Naturforsch.* **2019**, *74* (8), 697−707.
(40) Majeed, I.; Nadeem, M. A.; Al-Oufi, M.; Nadeem, M. A.; Waterhouse, G. I. N.; Badshah, A.; Metson, J. B.; Idriss, H. On the role of metal particle size and surface coverage for photo-catalytic hydrogen production; a case study of the Au/CdS system. *Applied Catalysis B. Environmental* **2016**, *182*, 266−276.
(41) Zhao, W.; Bajdich, M.; Carey, S.; Vojvodic, A.; Nørskov, J. K.; Campbell, C. T. Water Dissociative Adsorption on NiO(111): Energetics and Structure of the Hydroxylated Surface. *ACS Catal.* **2016**, *6*, 7377−7384.
(42) He, H.; Andersson, D. A.; Allred, D. D.; Rector, K. D. Determination of the Insulation Gap of Uranium Oxides by Spectroscopic Ellipsometry and Density Functional Theory. *J. Phys. Chem. C* **2013**, *117*, 16540−16551.
(43) Trasatti, S. The Absolute Electrode Potential: an Explanatory Note (Recommendations 1986), International Union of Pure and Applied Chemistry. *Pure & AppL Chem.* **1986**, *58*, 955−966.
(44) Lousada, C. M.; Johansson, A. J.; Brinck, T.; Jonsson, M. Mechanism of H_2O_2 Decomposition on Transition Metal Oxide Surfaces. *J. Phys. Chem. C* **2012**, *116*, 9533−9543.
(45) Cheng, J.; Vondele, J. V.; Sprik, M. Identifying Trapped Electronic Holes at the Aqueous TiO_2 Interface. *J. Phys. Chem. C* **2014**, *118*, 5437−5444.
(46) Tsuge, M.; Watanabe, N. Behavior of Hydroxyl Radicals on Water Ice at Low Temperatures. *Acc. Chem. Res.* **2021**, *54*, 471−480.
(47) Eriksen, S.; Naylor, P. D.; Egdell, R. G. Spectrochim. The adsorption of water on $SrTiO_3$ and TiO_2: a reappraisal. *Acta Part A* **1987**, *43*, 1535−1538.